Functional LCAT deficiency in human apolipoprotein A-I transgenic, SR-BI knockout mice

Ji-Young Lee,* Robert M. Badeau,* Anny Mulya,* Elena Boudyguina,* Abraham K. Gebre,* Thomas L. Smith,† and John S. Parks[1,*]

Department of Pathology/Section on Lipid Sciences* and Department of Orthopedic Surgery,† Wake Forest University School of Medicine, Winston-Salem, NC 27157

Abstract **Reduction of plasma LCAT activity has been observed in several conditions in which the size of HDL particles is increased; however, the mechanism of this reduction remains elusive. We investigated the plasma activity, mass, and in vivo catabolism of LCAT and its association with HDL particles in human apolipoprotein A-I transgenic, scavenger receptor class B type I knockout (*hA-I* ^{Tg} *SR-BI*$^{-/-}$) mice. Compared with *hA-I* ^{Tg} mice, *hA-I* ^{Tg} *SR-BI*$^{-/-}$ mice had a 4-fold higher total plasma cholesterol concentration, which occurred predominantly in 13–18 nm diameter HDL particles, a significant reduction in plasma esterified cholesterol-total cholesterol (EC/TC) ratio, and significantly lower plasma LCAT activity, suggesting a decrease in LCAT protein. However, LCAT protein in plasma, hepatic mRNA for LCAT, and in vivo turnover of ^{35}S-radiolabeled LCAT were similar in both genotypes of mice. HDL from *hA-I* ^{Tg} *SR-BI*$^{-/-}$ mice was enriched in sphingomyelin (SM), relative to phosphatidylcholine, and had less associated [^{35}S]LCAT radiolabel and endogenous LCAT activity compared with HDL from *hA-I* ^{Tg} mice. We conclude that the decreased EC/TC ratio in the plasma of *hA-I* ^{Tg} *SR-BI*$^{-/-}$ mice is attributed to a reduction in LCAT reactivity with SM-enriched HDL particles.**—Lee, J-Y., R. M. Badeau, A. Mulya, E. Boudyguina, A. K. Gebre, T. L. Smith, and J. S. Parks. **Functional LCAT deficiency in human apolipoprotein A-I transgenic, SR-BI knockout mice.** ***J. Lipid Res.*** **2007.** 48: **1052–1061.**

Supplementary key words high density lipoproteins • cholesterol • sphingomyelin • lecithin:cholesterol acyltransferase • scavenger receptor class B type I

Epidemiological studies have shown a strong inverse relationship between plasma HDL concentrations and the incidence of coronary heart disease. The antiatherogenic effect of HDL is likely attributable to several beneficial effects of HDL, including inhibition of cytokine-induced expression of adhesion molecules by endothelial cells (1), protection of LDLs from oxidation (2), and its ability to stimulate reverse cholesterol transport (3), a process in which excess cholesterol is removed from extrahepatic tissues and transported to the liver for excretion in the bile. As excess free cholesterol (FC) in peripheral tissues is added to the surface of HDL particles, it is esterified with a fatty acid molecule from phospholipid by the plasma enzyme LCAT, resulting in a more hydrophobic cholesteryl ester (CE) molecule that partitions into the core of the HDL particle. This process also leads to an increase in HDL particle size. The LCAT reaction is essential for the maturation of nascent HDL particles in plasma, and a genetic deficiency of LCAT results in the near absence of normal HDL particles and the presence of plasma very low density and low density lipoprotein particles of abnormal size and shape.

Scavenger receptor class B type I (SR-BI) was identified as the HDL receptor that mediates selective HDL CE uptake by the liver and steroidogenic tissues (4). Selective uptake of HDL CE was first suggested on the basis of CE uptake that exceeded that of HDL apolipoproteins (4–7). The physiological role of SR-BI in cholesterol metabolism and atherosclerosis development has been suggested by studies involving genetic ablation or overexpression of SR-BI in mice. SR-BI overexpression resulted in a decrease in plasma HDL cholesterol and an increase in biliary cholesterol concentration (8–10). Overexpression of SR-BI in LDL receptor knockout mice fed a high-fat/high-cholesterol diet strikingly reduced atherosclerotic lesions (11, 12). In contrast, SR-BI knockout (*SR-BI*$^{-/-}$) mice showed an increase in plasma cholesterol concentration and a decrease in gallbladder cholesterol (13, 14). In SR-BI and apolipoprotein E (apoE) double knockout

Manuscript received 21 September 2006 and in revised form 27 November 2006 and in re-revised form 30 January 2007 and in re-re-revised form 31 January 2007.

Published, JLR Papers in Press, February 1, 2007.
DOI 10.1194/jlr.M600417-JLR200

Abbreviations: apoE, apolipoprotein E; CE, cholesteryl ester; CETP, cholesteryl ester transfer protein; EC, esterified cholesterol; FC, free cholesterol; FPLC, fast-protein liquid chromatography; *hA-I* ^{Tg}, human apolipoprotein A-I transgenic; hrLCAT, human recombinant lecithin:cholesterol acyltransferase; PC, phosphatidylcholine; PLTP, phospholipid transfer protein; rHDL, recombinant high density lipoprotein; SM, sphingomyelin; SR-BI, scavenger receptor class B type I; TC, total cholesterol.

[1] To whom correspondence should be addressed.
e-mail: jparks@wfubmc.edu

mice, there were significant increases in plasma cholesterol concentration and extensive atherosclerosis compared with SR-BI or apoE single knockout mice, and the double knockout mice died of cardiovascular problems by 8 weeks of age (13, 15). Similarly, LDL receptor knockout mice fed an atherogenic diet with reduced hepatic SR-BI expression showed an increase in atherosclerosis (16). The mechanisms by which SR-BI exerts its atheroprotective effect remain unclear. Possible mechanisms include more favorable changes in plasma lipoprotein concentrations and composition, increased cholesterol flux out of the arterial wall, and increased selective CE uptake by the liver.

SR-BI$^{-/-}$ mice have enlarged plasma HDL particles that have an increase in the ratio of FC to total cholesterol (TC) and are enriched in apoE (14, 17). The increased FC/TC ratio in these mice has been suggested to result from a decrease in LCAT-mediated cholesterol esterification (18, 19). There are other experimental situations in which HDL enlargement is associated with decreased plasma LCAT activity. Fenofibrate treatment increased HDL particle size in both human apolipoprotein A-I transgenic (*hA-I* ^{Tg}) and C57BL/6 mice by increasing phospholipid transfer protein (PLTP) gene expression through a peroxisome proliferator-activated receptor α-dependent pathway (20), and plasma LCAT activity decreased as the dose of fenofibrate increased. The decrease in LCAT activity was mediated at the posttranscriptional level in *hA-I* ^{Tg} mice and at the transcriptional level in C57BL/6 mice. Human subjects with genetic cholesteryl ester transport protein (CETP) deficiency have an accumulation in plasma of enlarged HDL particles, enriched in apoE (21), and lower plasma cholesterol esterification rates compared with normal subjects, with no difference in LCAT mass, suggesting that a functional LCAT deficiency exists in these subjects (22). However, in a more recent study of homozygous CETP-deficient subjects, HDL_2 particles were observed to be enriched in LCAT and esterification rates of cholesterol in these particles were increased relative to HDL_2 particles from normal controls (23).

A systematic study to determine the relationship between HDL particle enlargement and LCAT activity has not been performed, and the mechanisms responsible for the decrease in LCAT activity with HDL particle enlargement, observed in past studies, have not been explored. To address these issues, we created a new mouse strain that maximized HDL particle size heterogeneity by crossing *SR-BI*$^{-/-}$ mice with *hA-I* ^{Tg}. The enlargement in HDL particle size manifested by the elimination of SR-BI was exacerbated by the overexpression of human apoA-I, resulting in the accumulation of very large HDL particles (13–18 nm diameter) in plasma. Our results demonstrate that plasma LCAT activity was reduced by 70% in *hA-I* ^{Tg} *SR-BI*$^{-/-}$ mice compared with *hA-I* ^{Tg} mice as a result of a decreased association of LCAT with enlarged HDL particles and not as a result of a decreased plasma LCAT mass, decreased hepatic LCAT gene expression, or increased LCAT catabolism in vivo.

METHODS

Animals

SR-BI$^{-/-}$ mice were kindly provided by Dr. David Williams (State University of New York at Stony Brook), and *hA-I* ^{Tg} mice were purchased from Charles River Laboratories (Wilmington, MA). Both strains of mice were in a mixed genetic background. *SR-BI*$^{+/-}$ (female) and *SR-BI*$^{-/-}$ (male) mice were crossed with *hA-I* ^{Tg} mice to generate *hA-I* ^{Tg} *SR-BI*$^{+/-}$ mice, which were then intercrossed to generate *hA-I* ^{Tg} *SR-BI*$^{+/+}$ (hereafter referred to as *hA-I* ^{Tg}), *hA-I* ^{Tg} *SR-BI*$^{+/-}$, and *hA-I* ^{Tg} *SR-BI*$^{-/-}$ mice. Genotypes were determined by genomic PCR of tail biopsies as described previously (24). Primer sequences used for genotyping were as follows: SR-BI wild-type allele (0.5 kb product), mSR-BI 13F (5′-TGTTTGCTGCGCTCGGCGTTG-3′) and mSR-BI 5R (5′-TATCCTCGGCAGACCTGAGTCGTGT-3′); SR-BI knockout allele (1.4 kb product), mSR-BI 3F (5′-TGAAGGTGGTCTTCAAGAGCAGTCCT-3′) and mSR-BI 4R (5′-GATTGGGAAGACAATAGCAGGCATGC-3′); and human apoA-I transgenic allele (1 kb product), AI-F Tg 3′ (5′-CAGCTCGTGCAGCTTCT-3′) and AI-R Tg 5′ (5′-TGAACCCCCCCAGAGCC-3′). The mice were housed in the Wake Forest University School of Medicine transgenic facility and maintained on a commercial diet (Prolab® RHM 3000). All protocols and procedures were approved by the Animal Care and Use Committee of the Wake Forest University School of Medicine.

Plasma lipid, lipoprotein, and apolipoprotein analyses

Mice were bled at 8–12 weeks of age after a 4 h fast to measure plasma lipid concentrations and to perform lipoprotein analyses. Plasma TC, FC, triglyceride, and phospholipid concentrations were determined by enzymatic analysis (Wako Chemicals) (25). Esterified cholesterol (EC) concentration was calculated as TC minus FC. HDL cholesterol was measured by enzymatic assay of the plasma supernatant after precipitation of apoB-containing lipoproteins with heparin-manganese (26). Human plasma apoA-I concentration was quantified by ELISA using monospecific antiserum to monkey as described previously (27).

Plasma lipoprotein distribution was determined by fast-protein liquid chromatography (FPLC). Pooled mouse plasma (150 μl) from each genotype was applied to two Superose 6 (1 × 30 cm) columns in series, and the TC concentration in each fraction (100 μl) was measured by enzymatic assay to obtain the lipoprotein cholesterol elution profile. Fractions were taken from the FPLC column for Western blot analysis using anti-human apoA-I and anti-mouse apoE primary polyclonal antibodies (Biodesign). The blots were developed using a horseradish peroxidase system (Pierce).

Analysis of plasma sphingomyelin and phosphatidylcholine content

Plasma from *hA-I* ^{Tg} and *hA-I* ^{Tg} *SR-BI*$^{-/-}$ mice was lipid-extracted, and the phospholipid classes were separated by thin-layer chromatography and assayed for phosphorus content as described previously (28), except that phosphatidylcholine (PC) and sphingomyelin (SM) bands from the thin-layer chromatography plate were analyzed directly for phosphorus (29) without prior lipid extraction from the silica gel. Blank lipid extracts were run as controls, and bands in the migration position of PC and SM were scraped and assayed for background color development. The blank extraction result was then subtracted from the corresponding PC or SM value.

Plasma LCAT, PLTP, and hepatic lipase (HL) activities

Plasma activities of LCAT, PLTP, and HL were measured using exogenous substrate as reported previously (30). Recombinant high density lipoprotein (rHDL) substrate particles for the exoge-

nous LCAT assay were made by cholate dialysis using 1-palmitoyl-2-arachidonyl-*sn*-glycero-3-phosphocholine, [^{3}H]cholesterol (50,000 dpm/μg), and apoA-I (80:5:1 molar ratio). Because of the 4-fold increase in plasma cholesterol in the *hA-I* ^{Tg} *SR-BI*$^{-/-}$ mice compared with *hA-I* ^{Tg} mice (see Results), the substrate concentration of rHDL cholesterol was increased from the routine value of 4 μM to 20 μM on the basis of pilot substrate saturation studies. The endogenous cholesterol esterification rate was measured by the method of Stokke and Norum (31).

Hepatic LCAT mRNA and plasma LCAT mass measurement

Hepatic LCAT mRNA abundance was measured by quantitative real-time PCR as described previously (26). Liver samples from *hA-I* ^{Tg} and *hA-I* ^{Tg} *SR-BI*$^{-/-}$ mice were quick-frozen in liquid N_2 and stored at −80°C until use. Total RNA was isolated from liver samples using TRIzol reagent (Invitrogen), and 1 μg of total RNA was reverse-transcribed using the Omniscript reverse transcript reagents (Qiagen) according to the manufacturer's instructions to synthesize cDNA. Real-time PCR was performed using SYBR Green Master Mix (Applied Biosystems) in an ABI Prism 7700 Detection System to measure LCAT and GAPDH mRNA abundance. Primers used were as follows: LCAT-forward, 5′-GCTGGCCTGGTAGAG-GAGATG-3′; LCAT-reverse, 5′-CCAAGGCTATGCCCAATGA-3′; GAPDH-forward, 5′-TGTGTCCGTCGTGGATCTGA-3′; and GAPDH-reverse, 5′-CCTGCTTCACCACCTTCTTGAT-3′. Data were analyzed using the $2^{-\Delta\Delta Ct}$ method (32).

Plasma samples (0.2 μl) from *hA-I* ^{Tg}, *hA-I* ^{Tg} *SR-BI*$^{-/-}$, and *LCAT*$^{-/-}$ mice (negative control) as well as purified mouse LCAT (33) were subjected to 4–16% SDS-PAGE followed by Western blot analysis using rabbit anti-mouse LCAT antiserum. LCAT was visualized using a horseradish peroxidase reagent (Pierce).

Isolation of ^{35}S-radiolabeled human recombinant LCAT

Human LCAT, radiolabeled with [^{35}S]methionine/cysteine, was produced and purified as described previously (34). Activity of the purified LCAT enzymes was measured using an exogenous substrate (30), protein content was quantified using a chemical assay (35), and ^{35}S radiolabel was determined by liquid scintillation spectroscopy. The specific activity of human LCAT was 4.6×10^5 cpm/μg LCAT protein. One microgram of [^{35}S]human recombinant lecithin:cholesterol acyltransferase (hrLCAT) protein was loaded on a 4–16% SDS-PAGE gel, and the LCAT protein was visualized by silver staining, Western blot analysis using rabbit anti-mouse LCAT antiserum, and phosphorimager analysis.

Association of endogenous mouse LCAT with plasma HDL

To determine the association of mouse LCAT mass and activity among plasma lipoproteins, 500 μl of plasma from *hA-I* ^{Tg} and *hA-I* ^{Tg} *SR-BI*$^{-/-}$ mice was injected onto FPLC Superose columns and 50 μl of each FPLC fraction was analyzed for LCAT activity using an exogenous rHDL substrate as described above.

Whole plasma from individual *hA-I* ^{Tg} and *hA-I* ^{Tg} *SR-BI*$^{-/-}$ mice was also fractionated on 4–30% nondenaturing gradient gels (36). The proteins were transferred to nitrocellulose and developed with rabbit anti-mouse LCAT or preimmune antiserum. Plasma from *LCAT*$^{-/-}$ mice and purified hrLCAT was run on the gels as negative and positive controls, respectively. Pilot experiments demonstrated that human LCAT cross-reacts with the rabbit anti-mouse LCAT antiserum.

In vivo kinetic study

An in vivo kinetic study was performed with ^{35}S-radiolabeled human LCAT using conditions similar to those described previously (36). Briefly, 2.5×10^5 cpm of the radiolabeled tracer was injected into the jugular vein of anesthetized recipient *hA-I* ^{Tg} and *hA-I* ^{Tg} *SR-BI*$^{-/-}$ mice. Blood samples were obtained by retro-orbital bleeding at 10 and 30 min and at 1, 2, 3, 5, 8, and 24 h after dose injection. Radioactivity of plasma samples was counted using a liquid scintillation counter to determine plasma decay of the tracer.

Plasma (500 μl) from the 24 h time point of the plasma die-away was fractionated by FPLC. Each fraction was assayed for cholesterol by enzymatic assay, for [^{35}S]LCAT radiolabel by liquid scintillation spectroscopy, and for LCAT activity using an exogenous rHDL substrate.

Statistical analysis

The results are expressed as means ± SD. Differences among the genotypes of mice were analyzed using one-way ANOVA, followed by Tukey's multiple comparison test to identify individual differences. All statistical analyses were performed using InStat software (GraphPad Software, Inc., San Diego, CA).

RESULTS

Plasma lipid and lipoprotein analyses of *hA-I* ^{Tg} *SR-BI*$^{-/-}$ mice

Plasma lipid and human apoA-I concentrations for chow-fed *hA-I* ^{Tg} *SR-BI*$^{-/-}$ mice at 8–12 weeks of age are shown in **Table 1**. Plasma TC, FC, and EC concentrations were 4.3-, 5.6-, and 3.9-fold higher in *hA-I* ^{Tg} *SR-BI*$^{-/-}$ mice compared with *hA-I* ^{Tg} mice. The EC/TC ratio was significantly lower in *hA-I* ^{Tg} *SR-BI*$^{-/-}$ mice compared with *hA-I* ^{Tg} mice, suggesting a possible defect in cholesterol esterification in the mice with inactive SR-BI. Plasma triglyceride and human apoA-I concentrations were similar among the three genotypes of mice.

To investigate the size distribution and apolipoprotein content of plasma lipoproteins, plasma samples from the mice were fractionated by FPLC, and apoA-I and apoE contents of the column fractions was determined by Western blot analysis. The FPLC profile of TC revealed marked enlargement of HDL particles in *hA-I* ^{Tg} *SR-BI*$^{-/-}$ mice, whereas *hA-I* ^{Tg} and *hA-I* ^{Tg} *SR-BI*$^{+/-}$ mice had similar FPLC profiles (**Fig. 1**). Nondenaturing gradient gel electrophoresis analysis showed that the enlarged HDL particles in the plasma of *hA-I* ^{Tg} *SR-BI*$^{-/-}$ mice were 13–18 nm in diameter (data not shown). Separation of plasma by agarose gel electrophoresis, followed by staining with Sudan black (30), demonstrated that all detectable lipoproteins in the plasma of the three genotypes of mice migrated in the α position, indicative of HDL (data not shown). The distribution of apoA-I for *hA-I* ^{Tg} mouse plasma was similar to that of cholesterol, and we found no evidence for another peak of HDL protein, indicative of small lipid-poor HDL particles, beyond fraction 66 (data not shown). However, the apoA-I distribution in *hA-I* ^{Tg} *SR-BI*$^{-/-}$ mouse plasma was skewed toward the larger HDL fractions (fractions 47–53) relative to that of *hA-I* ^{Tg} mouse plasma. The distribution of apoE was limited to the largest HDL particles (fractions 45–50) and appeared to be increased in the plasma of *hA-I* ^{Tg} *SR-BI*$^{-/-}$ mice compared with *hA-I* ^{Tg} mice (data not shown), consistent

with the findings of Rigotti et al. (14), who also observed enlarged HDL particles enriched in apoE in *SR-BI* knockout mice.

Activities of plasma HDL remodeling enzymes

To determine whether *hA-I* ^{Tg} *SR-BI*$^{-/-}$ mice had reduced plasma LCAT activity, we measured the plasma activities of LCAT and two other plasma HDL remodeling proteins, HL and PLTP, using exogenous substrates. Plasma LCAT activity in *hA-I* ^{Tg} *SR-BI*$^{-/-}$ mice was 28% of that in *hA-I* ^{Tg} mice (Table 1), suggesting that LCAT mass or specific activity in plasma may be reduced significantly. The endogenous cholesterol esterification rate in *hA-I* ^{Tg} *SR-BI*$^{-/-}$ mice was 13.8 ± 1.9% (mean ± SEM; n = 5 experiments) of that in *hA-I* ^{Tg} mice. When normalized for the 5.5-fold higher plasma FC concentration in *hA-I* ^{Tg} *SR-BI*$^{-/-}$ mice compared with *hA-I* ^{Tg} mice, a 40% reduction in absolute cholesterol esterification was observed (Table 1). HL and PLTP activities were similar between *hA-I* ^{Tg} and *hA-I* ^{Tg} *SR-BI*$^{-/-}$ mice (Table 1).

Hepatic LCAT mRNA and plasma LCAT protein measurements

Reduction of plasma LCAT activity in *hA-I* ^{Tg} *SR-BI*$^{-/-}$ mice using exogenous rHDL substrate could be attributable to several mechanisms, including decreased LCAT production, increased plasma LCAT turnover, or inhibition of LCAT activity by the large HDL particles in plasma. To investigate LCAT production in our mice, we analyzed hepatic LCAT mRNA by quantitative real-time PCR, because LCAT is synthesized and secreted by the liver. There was no significant difference in hepatic LCAT mRNA expression between *hA-I* ^{Tg} *SR-BI*$^{-/-}$ and *hA-I* ^{Tg} mice (**Fig. 2A**). This result is also in agreement with another study that reported no differences in hepatic LCAT mRNA expression in wild-type and *SR-BI*$^{-/-}$ mice (19, 37). In addition, Western blot analysis of plasma samples from four representative mice of each genotype showed that plasma LCAT mass was similar in these mice (Fig. 2B). These results indicate that reduced plasma LCAT activity in *hA-I* ^{Tg} *SR-BI*$^{-/-}$ mice was not attributable to changes in hepatic LCAT expression or plasma LCAT protein mass.

Plasma turnover of ^{35}S-labeled human LCAT

To determine whether plasma LCAT catabolism was affected in our mice, we measured the plasma decay of radiolabeled human LCAT in *hA-I* ^{Tg} and *hA-I* ^{Tg} *SR-BI*$^{-/-}$ recipient mice. Histidine-tagged human LCAT was radiolabeled metabolically with [^{35}S]methionine/cysteine and purified (34). The [^{35}S]hrLCAT tracer migrated with authentic LCAT, as judged by silver staining, Western blot, and phosphorimager analysis of the tracer after SDS-PAGE (**Fig. 3A**). The [^{35}S]hrLCAT tracer was injected into the jugular vein of recipient mice, and plasma decay of the radiolabel was followed for 24 h. Plasma die-away of [^{35}S]hrLCAT was similar in both genotypes of mice (Fig. 3B).

TABLE 1. Plasma measurements of *hA-I* ^{Tg} *SR-BI*$^{-/-}$ mice

Genotype	Total Plasma Cholesterol	Free Cholesterol	Esterified Cholesterol	Triglyceride	Human Apolipoprotein A-I	Esterified Cholesterol-Total Cholesterol Ratio	Esterified Cholesterol-Phosphatidylcholine Ratio	LCAT	HL	Phospholipid Transfer Protein	Endogenous LCAT
	mg/dl	*%*		*units of activity*							
hA-I ^{Tg} *SR-BI*$^{+/+}$	193^{a} ± 55 (19)	43^{a} ± 12 (16)	146^{a} ± 58 (13)	54 ± 45 (13)	399 ± 172 (20)	78^{a} ± 4 (13)	0.080^{a} ± 0.010 (4)	30.5^{a} ± 7.9 (18)	12 ± 2 (7)	14,294 ± 3,611 (7)	101.3 (2)
hA-I ^{Tg} *SR-BI*$^{+/-}$	287^{b} ± 62 (20)	72^{a} ± 21 (28)	235^{b} ± 50 (17)	59 ± 47 (21)	ND	78^{a} ± 3 (13)	ND	33.1^{a} ± 13.8 (5)	ND	ND	ND
hA-I ^{Tg} *SR-BI*$^{-/-}$	823^{c} ± 159 (19)	239^{b} ± 106 (25)	573^{b} ± 147 (19)	59 ± 41 (18)	440 ± 178 (14)	69^{b} ± 11 (13)	0.247^{b} ± 0.081 (4)	8.2^{b} ± 4.5 (20)	15 ± 3 (7)	16,445 ± 4,679 (7)	59.5 (2)

hA-I ^{Tg} *SR-BI*$^{-/-}$, human apolipoprotein A-I transgenic, scavenger receptor class B type I knockout; ND, not determined. Values shown are means ± SD. Number of mice is given in parentheses. Values in each column with a different superscript letter are significantly different at $P < 0.05$. Units of activity are nmol cholesteryl ester formed/h/ml plasma for LCAT activity measured with an exogenous recombinant HDL substrate and endogenous LCAT activity, μmol FA released/h/ml plasma for HL, and arbitrary units for PLTP.

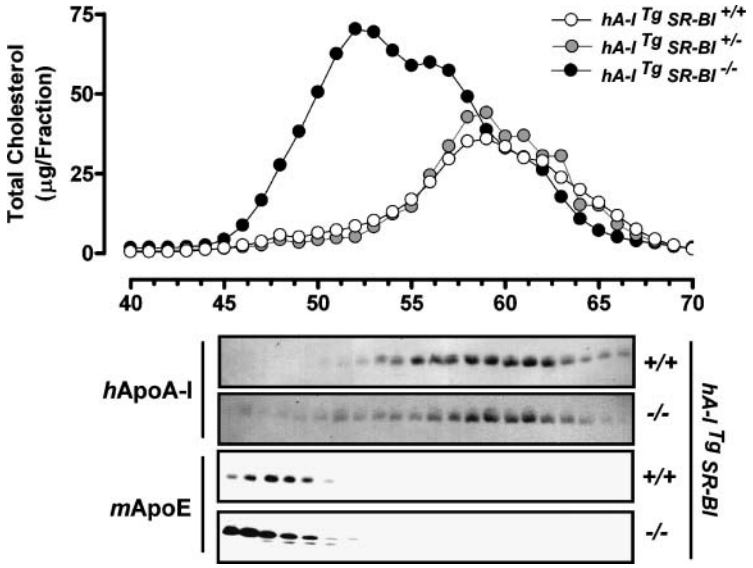

Fig. 1. Plasma lipoprotein and apolipoprotein analysis of human apolipoprotein A-I transgenic, scavenger receptor class B type I knockout (*hA-I* ^{Tg} *SR-BI*$^{-/-}$) mice. Plasma samples were obtained from 8–12 week old chow-fed mice of the indicated genotype after a 4 h fast. Plasma (150 μl) was fractionated on Superose 6 fast-protein liquid chromatography (FPLC) columns, and the total cholesterol (TC) concentration of each fraction was measured by enzymatic assay. An aliquot of fractions 45–66 was separated by SDS-PAGE, and the proteins were transferred to nitrocellulose. The nitrocellulose blots were then probed with anti-human apolipoprotein A-I (*h*ApoA-I) or anti-mouse apoE (*m*ApoE) antibodies and developed with horseradish peroxidase.

Association of LCAT with HDL particles

Because we did not observe any significant difference in hepatic LCAT mRNA abundance, plasma LCAT catabolism, or plasma LCAT mass between *hA-I* ^{Tg} and *hA-I* ^{Tg} *SR-BI*$^{-/-}$ mice, we explored the possibility that the decreased plasma LCAT activity observed in *hA-I* ^{Tg} *SR-BI*$^{-/-}$ mice might be attributed to decreased interaction of plasma LCAT with HDL particles. We tested this hypothesis by determining the mass distribution of plasma LCAT among HDL particles for three individual mice of both genotypes by fractionating plasma HDL on 4–30% nondenaturing gradient gels and probing for LCAT distribution with rabbit anti-mouse LCAT antiserum (**Fig. 4**). Plasma from *hA-I* ^{Tg} mice showed a rather diffuse distribution of LCAT in the 7.2–8.2 nm size range. However, plasma from *hA-I* ^{Tg} *SR-BI*$^{-/-}$ mice demonstrated a smaller, less diffuse band in the 7.2 nm size region of the gel that is smaller than most plasma HDL particles (30). Two controls demonstrated the specificity of the LCAT banding pattern between 7.2 and 8.2 nm: *1*) the lack of a LCAT band in that region in plasma from LCAT$^{-/-}$ mice; and *2*) no detectable band in that region when blots were developed with preimmune serum. These results suggested that plasma LCAT in *hA-I* ^{Tg} *SR-BI*$^{-/-}$ mice was not likely associated with HDL particles or with lipid-poor HDL.

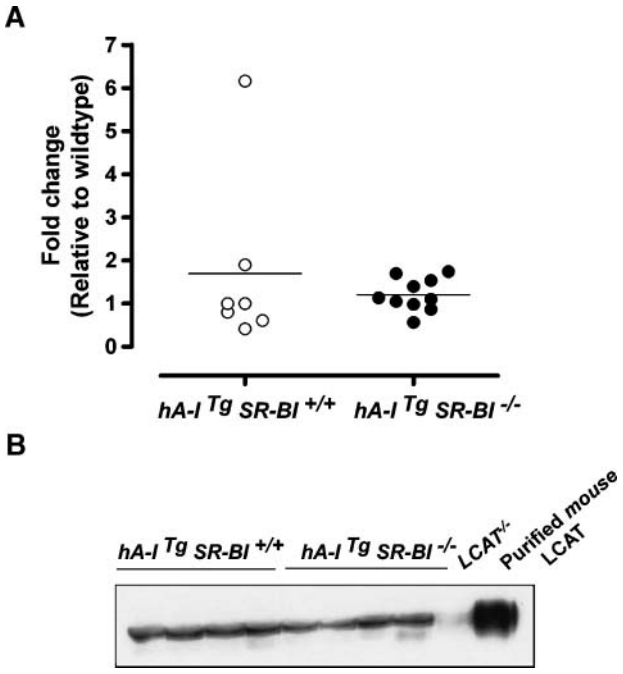

Fig. 2. Hepatic LCAT mRNA and plasma LCAT protein measurements in *hA-I* ^{Tg} and *hA-I* ^{Tg} *SR-BI*$^{-/-}$ mice. A: LCAT mRNA abundance in the livers of *hA-I* ^{Tg} and *hA-I* ^{Tg} *SR-BI*$^{-/-}$ mice. Total RNA was isolated from liver samples, and 1 μg was reverse-transcribed into cDNA. Quantitative real-time PCR was performed using SYBR Green. The data were normalized using GAPDH as an internal control and expressed as fold change relative to a *hA-I* ^{Tg} sample. The horizontal bars represent the mean values of the data points. B: Western blot analysis of plasma LCAT protein mass. Plasma samples (0.2 μl) from four *hA-I* ^{Tg} mice, four *hA-I* ^{Tg} *SR-BI*$^{-/-}$ mice, a *LCAT*$^{-/-}$ mouse, and purified mouse LCAT were fractionated on SDS-PAGE, and LCAT was detected by Western blot analysis using rabbit antiserum against mouse LCAT.

In vivo association of [^{35}S]LCAT with HDL particles

The in vivo association of [^{35}S]LCAT with plasma HDL was determined at the end of the turnover study for recipient mice by FPLC fractionation of the 24 h time point plasma, followed by quantification of radiolabel and cholesterol in each fraction. We also measured LCAT activity in each fraction using an exogenous rHDL substrate. Significantly more of the recovered [^{35}S]LCAT tracer was associated with normal-sized HDL particles (**Fig. 5A**, fractions 54–64; 7.5–12 nm diameter) in the terminal plasma samples of *hA-I* ^{Tg} mice compared with plasma from *hA-I* ^{Tg} *SR-BI*$^{-/-}$ mice (35.8 ± 2.0% vs. 26.0 ± 2.1%; mean ± SEM; n = 3, $P = 0.027$). This trend was also observed for the elution of mouse LCAT activity in the plasma samples; the mouse LCAT activity peak (Fig. 5B) and LCAT protein (data not shown) were shifted to the left in plasma of

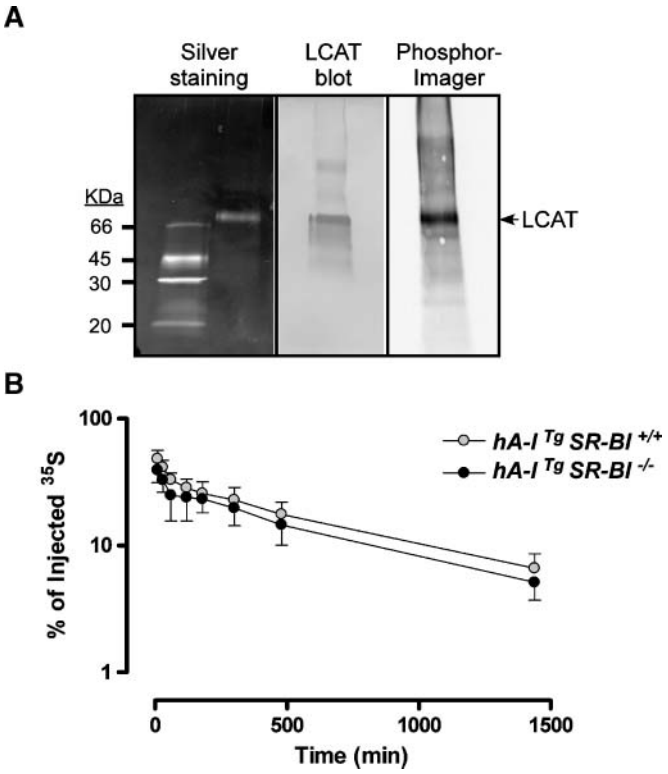

Fig. 3. In vivo catabolism of ^{35}S-labeled human recombinant lecithin:cholesterol acyltransferase (rhLCAT) in mice. A: Histidine-tagged ^{35}S-radiolabeled rhLCAT protein (1 μg) was subjected to electrophoresis on 4–16% SDS-PAGE gels, and LCAT was visualized by silver stain, Western blot with anti-human LCAT antiserum (LCAT blot), and phosphorimager analysis. The migration positions of low molecular weight marker proteins are indicated at left. B: Whole plasma die-away of ^{35}S-labeled rhLCAT tracer in *hA-I* ^{Tg} and *hA-I* ^{Tg} *SR-BI*$^{-/-}$ mice. [^{35}S]LCAT (2.5×10^5 cpm/mouse) was injected into the jugular vein of recipient mice, and blood samples were obtained over 24 h. The radioactivity of plasma samples was quantified in a γ counter and converted to percentage of injected radioactivity remaining at the indicated time points. Values are means ± SD (n = 3–4 per genotype).

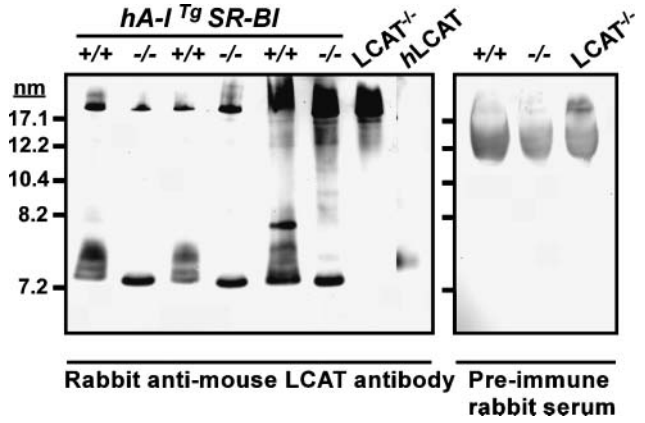

Fig. 4. Association of LCAT with HDL in plasma. Plasma samples for individual *hA-I* ^{Tg} and *hA-I* ^{Tg} *SR-BI*$^{-/-}$ mice were fractionated on 4–30% nondenaturing gradient gels. The proteins were then transferred to nitrocellulose paper, and LCAT was detected by Western blot analysis using rabbit anti-mouse LCAT antiserum (left panel) or preimmune antiserum (right panel). Plasma from a *LCAT*$^{-/-}$ mouse and rhLCAT, which cross-reacts with anti-mouse LCAT antiserum, was run as negative and positive controls, respectively. Hydrated diameter (nm) of standard proteins is shown at left of the blots. $^{+/+}$ and $^{-/-}$ denote the SR-BI genotypes of the mice.

hA-I ^{Tg} mice compared with that of *hA-I* ^{Tg} *SR-BI*$^{-/-}$ mice and overlapped more with the elution position of small HDL, suggesting that more LCAT was associated with HDL particles in *hA-I* ^{Tg} mice. The difference in the elution of human LCAT (Fig. 5A, fractions 56–62) and endogenous mouse LCAT activity (Fig. 5B, fractions 61–67) in the HDL region may represent a difference in HDL particle substrate preference for human and mouse LCAT or the fact that only a small percentage of the injected human LCAT remains in plasma after the 24 h turnover, and the remaining fraction of LCAT may not reflect the initial distribution of LCAT in plasma at earlier time points.

Enrichment of plasma with SM in *hA-I* ^{Tg} *SR-BI*$^{-/-}$ mice

An increase in plasma lipoprotein SM content has been shown to decrease plasma LCAT activity by decreasing the binding of LCAT to lipoprotein particle surfaces (38, 39). To determine whether an increase in plasma SM content might be responsible for less LCAT bound to HDL particles in *hA-I* ^{Tg} *SR-BI*$^{-/-}$ mouse plasma, we measured the SM/PC ratio in plasma (Table 1). There was a 3-fold increase ($P < 0.007$) in the SM/PC ratio in the plasma of *hA-I* ^{Tg} *SR-BI*$^{-/-}$ mice compared with *hA-I* ^{Tg} mice.

Association of rHDL [^{3}H]cholesterol with plasma HDL after LCAT assay

The results obtained to this point suggested that LCAT protein in *hA-I* ^{Tg} *SR-BI*$^{-/-}$ mouse plasma is not decreased relative to that in *hA-I* ^{Tg} mouse plasma, but its distribution is skewed toward the lipoprotein-free or lipid-poor HDL fraction of plasma. LCAT in the lipoprotein-free or lipid-poor HDL fraction of plasma should be reactive with rHDL; however, LCAT activity in *hA-I* ^{Tg} *SR-BI*$^{-/-}$ mouse plasma measured using rHDL was 28% of that in *hA-I* ^{Tg} mouse plasma (Table 1). To address this apparent paradox, we hypothesized that [^{3}H]cholesterol in rHDL substrate particles exchanged into large HDL particles in *hA-I* ^{Tg} *SR-BI*$^{-/-}$ mouse plasma during the LCAT assay, resulting in a decrease in measured LCAT activity attributable to the relatively poor reactivity of large HDL particles. To test this hypothesis, LCAT assays were performed using plasma from C57BL/6, *hA-I* ^{Tg}, and *hA-I* ^{Tg} *SR-BI*$^{-/-}$ mice or water (blank) as the LCAT source and rHDL as the exogenous substrate. After the assay, the incubation mixture was fractionated by FPLC and [^{3}H]cholesterol distribution in the eluted fractions was determined. Results for CE formation are shown in **Fig. 6A**. As anticipated, the CE formation rate for *hA-I* ^{Tg} *SR-BI*$^{-/-}$ plasma was 25% of that in *hA-I* ^{Tg} mouse plasma and the value for C57BL/6 plasma was intermediate. Fractionation of the incubation mixtures by FPLC showed that the elution

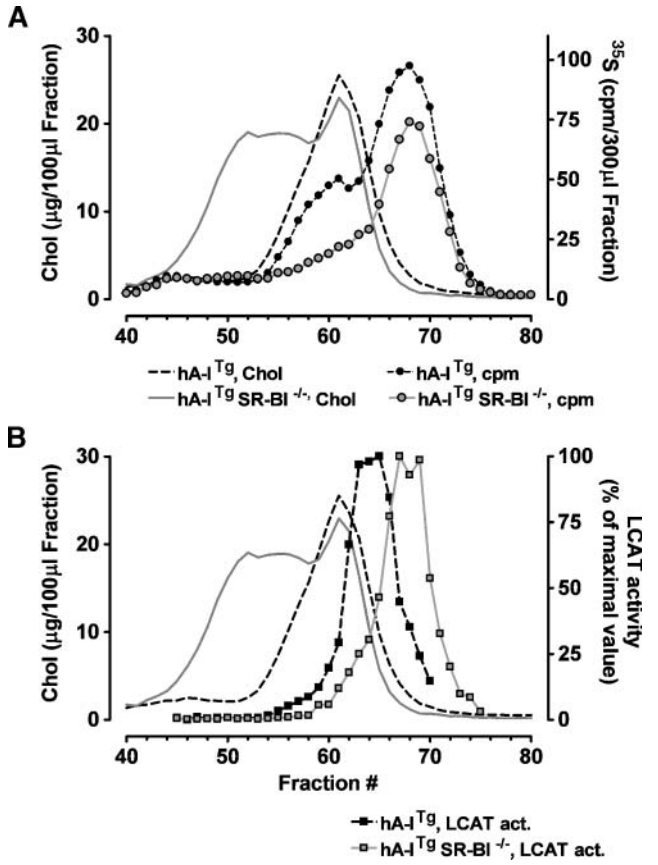

Fig. 5. Distribution of [^{35}S]rhLCAT protein and LCAT activity in FPLC fractions of plasma from *hA-I* ^{Tg} and *hA-I* ^{Tg} *SR-BI*$^{-/-}$ mice. Plasma samples (500 μl) collected at 24 h after injection of [^{35}S]LCAT into recipient mice (see Fig. 3) of the indicated genotypes were fractionated by FPLC. Fractions were collected for measurement of TC by enzymatic assay, [^{35}S]LCAT radiolabel distribution, and LCAT activity using an exogenous substrate assay. A: Cholesterol (Chol) mass and [^{35}S]LCAT radiolabel distribution. B: Cholesterol distribution and LCAT activity normalized to percentage of maximal activity for each column run.

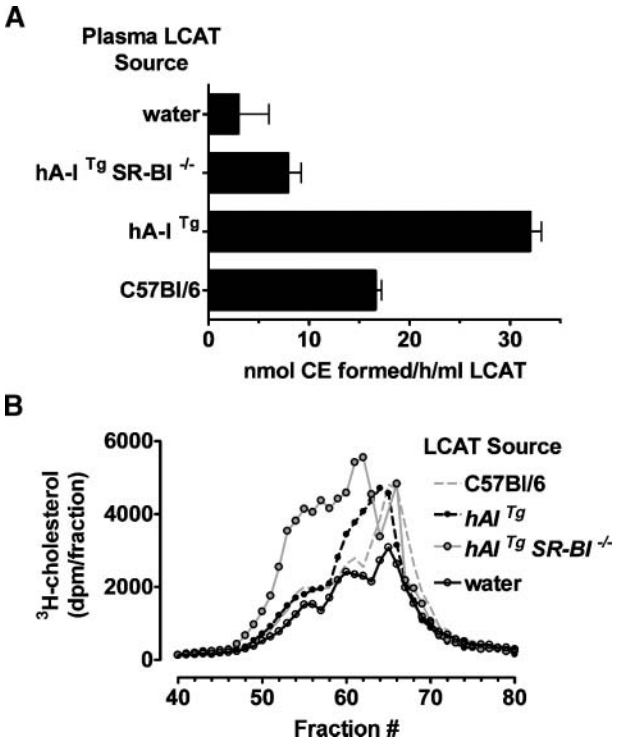

Fig. 6. Plasma LCAT assay using exogenous recombinant high density lipoprotein (rHDL) substrate. A: LCAT assay was performed with rHDL (80:5:1 molar ratio of 1-palmitoyl-2-arachidonyl-*sn*-glyero-3-phosphocholine, [^{3}H]cholesterol, and apoA-I) using plasma from *hA-I* ^{Tg}, *hA-I* ^{Tg} *SR-BI*$^{-/-}$, and C57BL/6 mice or water (control) as the source of LCAT protein, as described in Methods. Bars represent means of duplicate incubations, and error bars denote the range of the duplicates. CE, cholesteryl ester. B: Duplicate incubations of the LCAT assay described in A were fractionated by FPLC, and [^{3}H]cholesterol radiolabel was quantified in each fraction by liquid scintillation spectroscopy.

profile of rHDL radiolabel was similar for samples that used C57BL/6 and *hA-I* ^{Tg} mouse plasma as the LCAT source and paralleled that of the elution profile for rHDL incubated without plasma (i.e., water control) (Fig. 6B). However, the profile of rHDL radiolabel in the *hA-I* ^{Tg} *SR-BI*$^{-/-}$ plasma incubation was shifted to the left into a region of the column where large HDL particles elute. Fractions from the FPLC column were pooled and lipid-extracted, and FC and EC radiolabel were quantified. The pool corresponding to the large HDL elution region (fractions 46–56) contained 57% of the total [^{3}H]FC in the *hA-I* ^{Tg} *SR-BI*$^{-/-}$ plasma incubation but only 29, 17, and 16% in *hA-I* ^{Tg} plasma, C57BL/6 plasma, and water blank incubations, respectively. These data support the hypothesis that LCAT activity measured with rHDL substrate in *hA-I* ^{Tg} *SR-BI*$^{-/-}$ plasma is reduced compared with that in *hA-I* ^{Tg} plasma because the [^{3}H]cholesterol in the rHDL particles exchanges into the large HDL particles.

DISCUSSION

We have described a functional LCAT deficiency in a novel animal model (*hA-I* ^{Tg} *SR-BI*$^{-/-}$) that has extremely high plasma cholesterol concentrations (800 mg/dl). The relative LCAT deficiency manifests as a significant decrease in the EC/TC ratio in plasma and in LCAT activity, measured by an exogenous substrate assay. A similar observation has been made in other publications, in which the appearance of large HDL particles in plasma is described as accompanied by a decrease in the EC/TC ratio in plasma or a decrease in LCAT activity, suggesting that this could be a general response to the accumulation of large HDL in plasma (17, 20, 40, 41). However, the mechanism of the decreased LCAT activity in plasma has not been investigated. Our studies demonstrate that, despite a 70% decrease in plasma LCAT activity, plasma LCAT mass, hepatic mRNA for LCAT, and plasma catabolism of LCAT are similar between *hA-I* ^{Tg} and *hA-I* ^{Tg} *SR-BI*$^{-/-}$ mice. To explain this apparent paradox, we propose two possibilities. First, we provide evidence that LCAT is redistributed to the nonlipoprotein or lipid-poor HDL fraction of plasma in *hA-I* ^{Tg} *SR-BI*$^{-/-}$ mice and, therefore, is un-

available for cholesterol esterification on HDL particles. This could account for the decreased EC/TC ratio in the plasma of *hA-I* ^{Tg} *SR-BI*$^{-/-}$ mice relative to *hA-I* ^{Tg} mice. We hypothesized that the redistribution of LCAT in plasma was attributable to an accumulation of SM in HDL particles as a result of the lack of functional SR-BI. Previous studies have shown that SM enrichment of lipoproteins inhibits LCAT activity by preventing its binding to HDL (39), and analysis of the plasma SM content of *hA-I* ^{Tg} *SR-BI*$^{-/-}$ mice showed that the SM/PC ratio was increased by 3-fold relative to plasma of *hA-I* ^{Tg} mice. Second, the decrease in plasma LCAT activity measured by exogenous rHDL substrate appears to result from a redistribution of radiolabeled cholesterol from highly reactive rHDL particles to large (13–18 nm in diameter) HDL particles that are relatively unreactive with LCAT, resulting in an apparent decrease in LCAT activity in *hA-I* ^{Tg} *SR-BI*$^{-/-}$ mouse plasma. This study provides new insight into the mechanism of functional LCAT deficiency that occurs in *hA-I* ^{Tg} *SR-BI*$^{-/-}$ mice and may be applicable to other metabolic situations in which HDL particle size is increased.

Enlarged HDL particles, sometimes referred to as HDL_1, have also been observed in the plasma of several genetically altered mouse models (14, 17, 42–44), humans with CETP deficiency (22), and mice treated with fenofibrate (20), a ligand for the transcription factor peroxisome proliferator-activated receptor α. Fenofibrate appears to increase HDL particle size by inhibiting hepatic SR-BI expression (45, 46). In most of these studies, apoE enrichment of these enlarged HDL particles has been documented. Several of these studies have directly measured LCAT activity in plasma using exogenous rHDL substrate particles, whereas other studies have documented a decrease in the CE/TC ratio in plasma, suggesting a decrease in plasma LCAT. It was speculated that the decrease in plasma LCAT activity in one study resulted from decreased LCAT binding to HDL and increased catabolism of the enzyme (20). However, this hypothesis has never been tested directly, and no study has reported on the in vivo catabolism of LCAT.

We also obtained evidence for LCAT deficiency in a new mouse model that was generated by crossing SR-BI knockout mice with *hA-I* ^{Tg} mice to generate *hA-I* ^{Tg} *SR-BI*$^{-/-}$ mice. These mice had, in plasma, very high HDL concentrations, the appearance of apoE-enriched HDL_1 (Fig. 1), a significant decrease in EC/TC ratio, and a decrease in LCAT activity compared with *hA-I* ^{Tg} mice (Table 1). We hypothesized that the LCAT deficiency was attributable to increased plasma LCAT catabolism, as had been proposed in a previous publication (20). We found that plasma LCAT protein (Fig. 2B), hepatic mRNA for LCAT (Fig. 2A), and plasma decay of [^{35}S]rhLCAT (Fig. 3) were similar in both genotypes of mice, suggesting that our hypothesis was incorrect.

Previous studies have reported that 80–90% of LCAT in human plasma is bound to HDL particles (47). To explain our experimental results, we hypothesized that LCAT protein was redistributed to the nonlipoprotein fraction of plasma in *hA-I* ^{Tg} *SR-BI*$^{-/-}$ mice and was not available for the esterification of HDL FC. To test our hypothesis, we used two approaches. First, nondenaturing gradient gel electrophoresis showed a distinctly faster migration pattern for LCAT in a region of the gel that is smaller than α-migrating HDL particles, suggesting that less LCAT protein was associated with HDL in *hA-I* ^{Tg} *SR-BI*$^{-/-}$ mouse plasma (Fig. 4). Second, FPLC analysis of plasma demonstrated that relatively less [^{35}S]rhLCAT was associated with the HDL cholesterol peak in *hA-I* ^{Tg} *SR-BI*$^{-/-}$ mouse plasma compared with that in *hA-I* ^{Tg} mouse plasma (Fig. 5A). In addition, mouse LCAT activity in *hA-I* ^{Tg} *SR-BI*$^{-/-}$ mouse plasma, measured by an exogenous rHDL substrate, eluted in a later position compared with that of *hA-I* ^{Tg} mouse plasma and after the HDL cholesterol peak (Fig. 5B). Although these results can explain the decrease in plasma EC/TC ratio, they cannot explain why LCAT did not bind to normal-sized HDL particles, which are not decreased in *hA-I* ^{Tg} *SR-BI*$^{-/-}$ mouse plasma (Fig. 5, fractions 55–66), or why LCAT activity, measured with rHDL substrate particles, was low in *hA-I* ^{Tg} *SR-BI*$^{-/-}$ mouse plasma.

To explain the redistribution of LCAT in *hA-I* ^{Tg} *SR-BI*$^{-/-}$ mouse plasma, we hypothesized that the SM content of plasma HDL was increased. Several studies have shown that increasing the SM content of lipoproteins inhibits LCAT activity and that this inhibition is attributable to decreased binding of LCAT to lipoprotein surfaces enriched in SM (38, 39). In our study, we observed a 3-fold increase in the SM/PC ratio in *hA-I* ^{Tg} *SR-BI*$^{-/-}$ mouse plasma compared with *hA-I* ^{Tg} plasma, supporting the hypothesis that enrichment of HDL particles in plasma results in a redistribution of LCAT to the nonlipoprotein fraction of plasma. SR-BI has been reported to transfer SM from lipoproteins into cells, and this may represent an important pathway for the clearance of plasma SM (48, 49). The absence of functional SR-BI could result in the enrichment of HDL SM, which could be exchanged among HDL particles in plasma by PLTP (50), resulting in the net enrichment of SM in all plasma lipoprotein particles. This, in turn, could lead to decreased binding of LCAT to lipoproteins and less cholesterol esterification in plasma. An alternative explanation for our data may be that the absence of SR-BI leads to a unique perturbation of HDL particle structure that results in inhibition of LCAT binding and activity unrelated to the increase in SM.

In previous studies, LCAT activity in human plasma was highly correlated with LCAT mass (51). This has led to the practice of equating LCAT activity, determined with exogenous rHDL substrate particles, with the relative amount of LCAT protein in plasma. However, this assumption has not been adequately tested in plasma samples with high concentrations of HDL or enlarged HDL particles. Our results suggest that radiolabeled cholesterol in highly reactive rHDL particles exchanges into larger, less reactive HDL particles during the incubation, resulting in the measurement of less LCAT activity (Fig. 6). This result was verified using an endogenous LCAT assay in which radiolabeled cholesterol is incorporated into endogenous lipoproteins in plasma (31, 52). In five independent experiments, the percentage endogenous esterification rate for plasma from *hA-I* ^{Tg} *SR-BI*$^{-/-}$ mice was 13.8 ± 1.9%

(mean ± SEM) of that in plasma from *hA-I* ^{Tg} mice. In two of those experiments in which plasma FC was measured, the absolute endogenous cholesterol esterification rate in *hA-I* ^{Tg} *SR-BI* $^{-/-}$ mouse plasma was 60% of that observed in *hA-I* ^{Tg} mouse plasma (Table 1). These results suggest that in spite of a 5.5-fold increase in plasma FC concentration in *hA-I* ^{Tg} *SR-BI* $^{-/-}$ mouse plasma (Table 1), there was a deficiency in LCAT-mediated CE formation relative to *hA-I* ^{Tg} mouse plasma. Whether the decrease in LCAT-mediated cholesterol esterification is a phenotype of other genetically altered mouse models that have high HDL concentrations or an increase in the concentration of large HDL particles is unknown. However, our results suggest caution in interpreting lower than normal LCAT activity in the plasma of mice with increased HDL concentrations without supportive data regarding LCAT protein mass.

Enlarged HDL particles have been referred to as "dysfunctional" because of their association with increased atherosclerosis as well as ovarian dysfunction (18, 53). The exact nature of the particle that causes the dysfunction is poorly defined, but a recent study suggests that it may not be the size of the HDL particle per se but the increase in FC that is critical to the dysfunction (18). The increase in HDL FC may prevent cellular cholesterol efflux to HDL, because the FC chemical gradient that drives FC flux from cells to HDL is lost. Evidence from several studies suggests that the increase in HDL FC is not the result of LCAT deficiency in plasma. In one study, LCAT mass was normal in *SR-BI* $^{-/-}$ mouse plasma (19). In another study, a 10-fold overexpression of LCAT in *SR-BI* $^{-/-}$ mice had a minor effect on the FC/TC ratio and did not correct the ovarian dysfunction (18). Finally, overexpression of LCAT actually resulted in dysfunctional HDL (53). The results from all of these studies suggest that LCAT protein is present in plasma but unable to bind to HDL particles. Our results as well as previous studies indicate that this may be attributable to an increased SM content of HDL preventing LCAT binding to HDL surfaces (38, 39). In support of this idea is a recent study in which HDL_2 particles from CETP-deficient subjects were observed to have increased ABCG1-mediated cholesterol efflux from macrophages that was dependent on LCAT activity (23). The HDL_2 particles from CETP-deficient subjects had 10-fold more LCAT and a 50% reduction in SM/PC ratio compared with their normal counterparts. Thus, dysfunctional HDL particles may result in metabolic conditions in which the SM content of HDL is increased, resulting in decreased LCAT-mediated cholesterol esterification and increased HDL FC.

This work was supported by National Institutes of Health Grants HL-054176 and HL-049373 to J.S.P.

REFERENCES

1. Barter, P. J. 1997. Inhibition of endothelial cell adhesion molecule expression by high density lipoproteins. *Clin. Exp. Pharmacol. Physiol.* **24:** 286–287.
2. Parthasarathy, S., J. Barnett, and L. G. Fong. 1990. High-density lipoprotein inhibits the oxidative modification of low-density lipoprotein. *Biochim. Biophys. Acta.* **1044:** 275–283.
3. Glomset, J. A. 1968. The plasma lecithin:cholesterol acyltransferase reaction. *J. Lipid Res.* **9:** 155–167.
4. Acton, S., A. Rigotti, K. T. Landschulz, S. Xu, H. H. Hobbs, and M. Krieger. 1996. Identification of scavenger receptor SR-BI as a high density lipoprotein receptor. *Science.* **271:** 518–520.
5. Stein, Y., Y. Dabach, G. Hollander, G. Halperin, and O. Stein. 1983. Metabolism of HDL-cholesteryl ester in the rat, studied with a nonhydrolyzable analog, cholesteryl linoleyl ether. *Biochim. Biophys. Acta.* **752:** 98–105.
6. Krieger, M. 1999. Charting the fate of the "good cholesterol": identification and characterization of the high-density lipoprotein receptor SR-BI. *Annu. Rev. Biochem.* **68:** 523–558.
7. Krieger, M. 1998. The "best" of cholesterols, the "worst" of cholesterols: a tale of two receptors. *Proc. Natl. Acad. Sci. USA.* **95:** 4077–4080.
8. Ueda, Y., L. Royer, E. Gong, J. Zhang, P. N. Cooper, O. Francone, and E. M. Rubin. 1999. Lower plasma levels and accelerated clearance of high density lipoprotein (HDL) and non-HDL cholesterol in scavenger receptor class B type I transgenic mice. *J. Biol. Chem.* **274:** 7165–7171.
9. Wang, N., T. Arai, Y. Ji, F. Rinninger, and A. R. Tall. 1998. Liver-specific overexpression of scavenger receptor BI decreases levels of very low density lipoprotein apoB, low density lipoprotein apoB, and high density lipoprotein in transgenic mice. *J. Biol. Chem.* **273:** 32920–32926.
10. Kozarsky, K. F., M. H. Donahee, A. Rigotti, S. N. Iqbal, E. R. Edelman, and M. Krieger. 1997. Overexpression of the HDL receptor SR-BI alters plasma HDL and bile cholesterol levels. *Nature.* **387:** 414–417.
11. Kozarsky, K. F., M. H. Donahee, J. M. Glick, M. Krieger, and D. J. Rader. 2000. Gene transfer and hepatic overexpression of the HDL receptor SR-BI reduces atherosclerosis in the cholesterol-fed LDL receptor-deficient mouse. *Arterioscler. Thromb. Vasc. Biol.* **20:** 721–727.
12. Arai, T., N. Wang, M. Bezouevski, C. Welch, and A. R. Tall. 1999. Decreased atherosclerosis in heterozygous low density lipoprotein receptor-deficient mice expressing the scavenger receptor BI transgene. *J. Biol. Chem.* **274:** 2366–2371.
13. Trigatti, B., H. Rayburn, M. Vinals, A. Braun, H. Miettinen, M. Penman, M. Hertz, M. Schrenzel, L. Amigo, A. Rigotti, et al. 1999. Influence of the high density lipoprotein receptor SR-BI on reproductive and cardiovascular pathophysiology. *Proc. Natl. Acad. Sci. USA.* **96:** 9322–9327.
14. Rigotti, A., B. L. Trigatti, M. Penman, H. Rayburn, J. Herz, and M. Krieger. 1997. A targeted mutation in the murine gene encoding the high density lipoprotein (HDL) receptor scavenger receptor class B type I reveals its key role in HDL metabolism. *Proc. Natl. Acad. Sci. USA.* **94:** 12610–12615.
15. Braun, A., B. L. Trigatti, M. J. Post, K. Sato, M. Simons, J. M. Edelberg, R. D. Rosenberg, M. Schrenzel, and M. Krieger. 2002. Loss of SR-BI expression leads to the early onset of occlusive atherosclerotic coronary artery disease, spontaneous myocardial infarctions, severe cardiac dysfunction, and premature death in apolipoprotein E-deficient mice. *Circ. Res.* **90:** 270–276.
16. Huszar, D., M. L. Varban, F. Rinninger, R. Feeley, T. Arai, V. Fairchild-Huntress, M. J. Donovan, and A. R. Tall. 2000. Increased LDL cholesterol and atherosclerosis in LDL receptor-deficient mice with attenuated expression of scavenger receptor B1. *Arterioscler. Thromb. Vasc. Biol.* **20:** 1068–1073.
17. Van Eck, M., J. Twisk, M. Hoekstra, B. T. Van Rij, C. A. Van der Lans, I. S. Bos, J. K. Kruijt, F. Kuipers, and T. J. Van Berkel. 2003. Differential effects of scavenger receptor BI deficiency on lipid metabolism in cells of the arterial wall and in the liver. *J. Biol. Chem.* **278:** 23699–23705.
18. Yesilaltay, A., M. G. Morales, L. Amigo, S. Zanlungo, A. Rigotti, S. L. Karackattu, M. H. Donahee, K. F. Kozarsky, and M. Krieger. 2006. Effects of hepatic expression of the high-density lipoprotein receptor SR-BI on lipoprotein metabolism and female fertility. *Endocrinology.* **147:** 1577–1588.
19. Ma, K., T. Forte, J. D. Otvos, and L. Chan. 2005. Differential additive effects of endothelial lipase and scavenger receptor-class B type I on high-density lipoprotein metabolism in knockout mouse models. *Arterioscler. Thromb. Vasc. Biol.* **25:** 149–154.
20. Bouly, M., D. Masson, B. Gross, X. C. Jiang, C. Fievet, G. Castro, A. R. Tall, J. C. Fruchart, B. Staels, L. Lagrost, et al. 2001. Induction

of the phospholipid transfer protein gene accounts for the high density lipoprotein enlargement in mice treated with fenofibrate. *J. Biol. Chem.* **276:** 25841–25847.
21. Yamashita, S., D. L. Sprecher, N. Sakai, Y. Matsuzawa, S. Tarui, and D. Y. Hui. 1990. Accumulation of apolipoprotein E-rich high density lipoproteins in hyperalphalipoproteinemic human subjects with plasma cholesteryl ester transfer protein deficiency. *J. Clin. Invest.* **86:** 688–695.
22. Oliveira, H. C., L. Ma, R. Milne, S. M. Marcovina, A. Inazu, H. Mabuchi, and A. R. Tall. 1997. Cholesteryl ester transfer protein activity enhances plasma cholesteryl ester formation. Studies in CETP transgenic mice and human genetic CETP deficiency. *Arterioscler. Thromb. Vasc. Biol.* **17:** 1045–1052.
23. Matsuura, F., N. Wang, W. Chen, X-c. Jiang, and A. R. Tall. 2006. HDL from CETP-deficient subjects shows enhanced ability to promote cholesterol efflux from macrophages in an apoE- and ABCG1-dependent pathway. *J. Clin. Invest.* **116:** 1435–1442.
24. Furbee, J. W., Jr., O. L. Francone, and J. S. Parks. 2001. Alteration of plasma HDL cholesteryl ester composition with transgenic expression of a point mutation (E149A) of human lecithin:cholesterol acyltransferase (LCAT). *J. Lipid Res.* **42:** 1626–1635.
25. Carr, T. P., C. J. Andresen, and L. L. Rudel. 1993. Enzymatic determination of triglyceride, free cholesterol, and total cholesterol in tissue lipid extracts. *Clin. Biochem.* **26:** 39–42.
26. Timmins, J. M., J. Y. Lee, E. Boudyguina, K. D. Kluckman, L. R. Brunham, A. Mulya, A. K. Gebre, J. M. Coutinho, P. L. Colvin, T. L. Smith, et al. 2005. Targeted inactivation of hepatic Abca1 causes profound hypoalphalipoproteinemia and kidney hypercatabolism of apoA-I. *J. Clin. Invest.* **115:** 1333–1342.
27. Koritnik, D. L., and L. L. Rudel. 1983. Measurement of apolipoprotein A-I concentration in nonhuman primate serum by enzyme-linked immunosorbent assay (ELISA). *J. Lipid Res.* **24:** 1639–1645.
28. Parks, J. S., and A. K. Gebre. 1991. Studies on the effect of dietary fish oil on the physical and chemical properties of low density lipoproteins in cynomolgus monkeys. *J. Lipid Res.* **32:** 305–315.
29. Fiske, C. H., and Y. SubbaRow. 1925. Colorimetric determination of phosphorus. *J. Biol. Chem.* **66:** 357–400.
30. Lee, J. Y., J. M. Timmins, A. Mulya, T. L. Smith, Y. Zhu, E. M. Rubin, J. W. Chisholm, P. L. Colvin, and J. S. Parks. 2005. HDLs in apoA-I transgenic Abca1 knockout mice are remodeled normally in plasma but are hypercatabolized by the kidney. *J. Lipid Res.* **46:** 2233–2245.
31. Stokke, K. T., and K. R. Norum. 1971. Determination of lecithin:cholesterol acyltransfer in human blood plasma. *Scand. J. Clin. Lab. Invest.* **27:** 21–27.
32. Livak, K. J., and T. D. Schmittgen. 2001. Analysis of relative gene expression data using real-time quantitative PCR and the 2 (-Delta Delta C(T)) method. *Methods.* **25:** 402–408.
33. Zhao, Y., F. E. Thorngate, K. H. Weisgraber, D. L. Williams, and J. S. Parks. 2005. Apolipoprotein E is the major physiological activator of lecithin-cholesterol acyltransferase (LCAT) on apolipoprotein B lipoproteins. *Biochemistry.* **44:** 1013–1025.
34. Chisholm, J. W., A. K. Gebre, and J. S. Parks. 1999. Characterization of C-terminal histidine-tagged human recombinant lecithin:cholesterol acyltransferase. *J. Lipid Res.* **40:** 1512–1519.
35. Lowry, O. H., N. J. Rosebrough, A. J. Farr, and R. J. Randall. 1951. Protein measurement with the Folin phenol reagent. *J. Biol. Chem.* **193:** 265–275.
36. Lee, J. Y., L. Lanningham-Foster, E. Y. Boudyguina, T. L. Smith, E. R. Young, P. L. Colvin, M. J. Thomas, and J. S. Parks. 2004. Prebeta high density lipoprotein has two metabolic fates in human apolipoprotein A-I transgenic mice. *J. Lipid Res.* **45:** 716–728.
37. Mardones, P., V. Quinones, L. Amigo, M. Moreno, J. F. Miquel, M. Schwarz, H. E. Miettinen, B. Trigatti, M. Krieger, S. VanPatten, et al. 2001. Hepatic cholesterol and bile acid metabolism and intestinal cholesterol absorption in scavenger receptor class B type I-deficient mice. *J. Lipid Res.* **42:** 170–180.
38. Subbaiah, P. V., and M. Liu. 1993. Role of sphingomyelin in the regulation of cholesterol esterification in the plasma lipoproteins. Inhibition of lecithin-cholesterol acyltransferase reaction. *J. Biol. Chem.* **268:** 20156–20163.
39. Bolin, D. J., and A. Jonas. 1996. Sphingomyelin inhibits the lecithin-cholesterol acyltransferase reaction with reconstituted high density lipoproteins by decreasing enzyme binding. *J. Biol. Chem.* **271:** 19152–19158.
40. Ehnholm, S., K. W. van Dijk, B. Van't Hof, A. Van der Zee, V. M. Olkkonen, M. Jauhiainen, M. Hofker, L. Havekes, and C. Ehnholm. 1998. Adenovirus mediated overexpression of human phospholipid transfer protein alters plasma HDL levels in mice. *J. Lipid Res.* **39:** 1248–1253.
41. Moore, R. E., M. Navab, J. S. Millar, F. Zimetti, S. Hama, G. H. Rothblat, and D. J. Rader. 2005. Increased atherosclerosis in mice lacking apolipoprotein A-I attributable to both impaired reverse cholesterol transport and increased inflammation. *Circ. Res.* **97:** 763–771.
42. Wolfrum, C., M. N. Poy, and M. Stoffel. 2005. Apolipoprotein M is required for pre[beta]-HDL formation and cholesterol efflux to HDL and protects against atherosclerosis. *Nat. Med.* **11:** 418–422.
43. Foger, B., M. Chase, M. J. Amar, B. L. Vaisman, R. D. Shamburek, B. Paigen, J. Fruchart-Najib, J. A. Paiz, C. A. Koch, R. F. Hoyt, et al. 1999. Cholesteryl ester transfer protein corrects dysfunctional high density lipoproteins and reduces aortic atherosclerosis in lecithin cholesterol acyltransferase transgenic mice. *J. Biol. Chem.* **274:** 36912–36920.
44. Gruen, M. L., M. R. Plummer, W. Zhang, K. A. Posey, M. Linton, S. Fazio, and A. H. Hasty. 2005. Persistence of high density lipoprotein particles in obese mice lacking apolipoprotein A-I. *J. Lipid Res.* **46:** 2007–2014.
45. Fu, T., K. F. Kozarsky, and J. Borensztajn. 2003. Overexpression of SR-BI by adenoviral vector reverses the fibrate-induced hypercholesterolemia of apolipoprotein E-deficient mice. *J. Biol. Chem.* **278:** 52559–52563.
46. Mardones, P., A. Pilon, M. Bouly, D. Duran, T. Nishimoto, H. Arai, K. F. Kozarsky, M. Altayo, J. F. Miquel, G. Luc, et al. 2003. Fibrates down-regulate hepatic scavenger receptor class B type I protein expression in mice. *J. Biol. Chem.* **278:** 7884–7890.
47. Cheung, M. C., A. C. Wolf, K. D. Lum, J. H. Tollefson, and J. J. Albers. 1986. Distribution and localization of lecithin:cholesterol acyltransferase and cholesteryl ester transfer activity in A-I-containing lipoproteins. *J. Lipid Res.* **27:** 1135–1144.
48. Urban, S., S. Zieseniss, M. Werder, H. Hauser, R. Budzinski, and B. Engelmann. 2000. Scavenger receptor BI transfers major lipoprotein-associated phospholipids into the cells. *J. Biol. Chem.* **275:** 33409–33415.
49. Rodrigueza, W. V., S. T. Thuahnai, R. E. Temel, S. Lund-Katz, M. C. Phillips, and D. L. Williams. 1999. Mechanism of scavenger receptor class B type I-mediated selective uptake of cholesteryl esters from high density lipoprotein to adrenal cells. *J. Biol. Chem.* **274:** 20344–20350.
50. Rao, R., J. J. Albers, G. Wolfbauer, and H. J. Pownall. 1997. Molecular and macromolecular specificity of human plasma phospholipid transfer protein. *Biochemistry.* **36:** 3645–3653.
51. Albers, J. J., C. H. Chen, and J. L. Adolphson. 1981. Lecithin:cholesterol acyltransferase (LCAT) mass: its relationship to LCAT activity and cholesterol esterification rate. *J. Lipid Res.* **22:** 1206–1213.
52. Parks, J. S., A. K. Gebre, and J. W. Furbee, Jr. 1998. Lecithin-cholesterol acyltransferase. Assay of cholesterol esterification and phospholipase A2 activities. In Methods in Molecular Biology. M. Doolittle and K. Reue, editors. Humana Press, Totowa, NJ. 123–131.
53. Foger, B., M. Chase, M. J. Amar, B. L. Vaisman, R. D. Shamburek, B. Paigen, J. Fruchart-Najib, J. A. Paiz, C. A. Koch, R. F. Hoyt, et al. 1999. Cholesteryl ester transfer protein corrects dysfunctional high density lipoproteins and reduces aortic atherosclerosis in lecithin cholesterol acyltransferase transgenic mice. *J. Biol. Chem.* **274:** 36912–36920.